Visible-Light-Driven N−F−Codoped TiO_2 Photocatalysts. 2. Optical Characterization, Photocatalysis, and Potential Application to Air Purification

Di Li,* Hajime Haneda, Shunichi Hishita, and Naoki Ohashi

Advanced Materials Laboratory, National Institute for Materials Science (NIMS), 1-1 Namiki, Tsukuba, Ibaraki 305-0044, Japan

Received June 6, 2004. Revised Manuscript Received March 11, 2005

N−F−codoped TiO_2 (NFT) powders, prepared by spray pyrolysis (SP), were further characterized by ultraviolet−visible (UV−Vis) absorption spectroscopy and photoluminescence (PL) spectra. The UV−Vis spectra indicated that the NFT powders could absorb not only ultraviolet light like pure TiO_2 powder but also part of the visible-light spectrum ($\lambda < 550$ nm). The PL spectra provided confirmation that four electronic energy states exist between the valence band and conduction band of N−F−codoped TiO_2 that were attributed to *F* center, F^+ center, an origin-unidentified energy state, and an impurity energy state formed by doped N atoms. Acetaldehyde decomposition was used as a probe reaction to evaluate the photocatalytic properties of these NFT powders. As a result, we found that the photocatalytic activity of the NFT powder prepared at the SP temperature of 1173 K was superior to that of commercial P25 under both UV and Vis irradiation. Moreover, trichloroethylene and toluene were selected as the other two target reactants. Their decompositions on the optimal NFT powder were investigated using a specially designed reactor cell by simulating a commercial blue LED air cleaner. The results indicate that our SP sample has a good potential for application to air purification.

1. Introduction

N−F−codoped TiO_2 (NFT) powders were prepared by spray pyrolysis (SP) as described in part 1 with the aim of introducing new active sites by F-doping while the visible-light (Vis) absorption was improved by N-doping. As a result, a highly reactive, Vis-driven photocatalysis would be achieved.[1]

The Vis-driven photocatalysis of N-doped TiO_2 powders has been confirmed by many studies.[2−5] However, the mechanism for exhibiting Vis activity in this system is still an open question. It is quite debatable whether doped N atoms or oxygen vacancies, originated from N-doping, contribute to the Vis activity. Asahi et al. claimed that the doped N atoms narrow the band gap of TiO_2 and thus make it capable of absorbing visible light and exhibiting Vis-driven photocatalysis.[3] Irie et al. argued that the isolated narrow band formed above the valence band is responsible for the Vis response.[4] However, Ihara et al. insisted that it is the oxygen vacancies that contributed to the Vis activity and that the doped N atoms only enhance the stabilization of these oxygen vacancies.[5] Nakamura et al. also confirmed this role of oxygen vacancies in the plasma-treated TiO_2 photocatalysts.[6] In addition, Vis photocatalytic activity caused by the structural oxygen vacancy was also reported by Martyanov et al.[7]

As for the F−TiO_2 system, Minero et al. studied the photocatalytic decomposition of phenol in aqueous solution over fluorinated TiO_2 and claimed that the enhancement effect was mainly caused by an increase in the number of hydroxyl ($OH^•$) radicals since their formation was favored on fluorinated TiO_2.[8−10] Yu et al. studied the photocatalytic decomposition of gas-phase acetone over F-doped TiO_2. They proposed that the doped F atoms convert Ti^{4+} to Ti^{3+} by charge compensation and that the existence of a certain amount of Ti^{3+} reduces the electron−hole recombination rate and further enhances the photocatalytic activity.[11] Their different explanations are not surprising because the photocatalysts they used had pronounced differences in properties. For the fluorinated TiO_2, the fluorination was realized by adding NaF to the reaction solution containing TiO_2, i.e., by making the added fluoride react with the hydroxyl groups on the surface of TiO_2 to form ≡Ti−F species.[8−10] Obviously, the added F atoms only presented on the surface of TiO_2; this on-the-spot fluorination is only used for a liquid-

* Corresponding author. Tel.: +81-29-851-3354 ext. 8608. Fax: +81-29-855-1196. E-mail: LI.Di@nims.go.jp.

(1) Li, D.; Haneda, H.; Hishita, S.; Ohashi, N. *Chem. Mater.* **2005**, *17*, 2588.
(2) Sato, S. *Chem. Phys. Lett.* **1986**, *123* (12), 126.
(3) Asahi, R.; Morikawa, T.; Ohwaki, T.; Aoki, K.; Taga, Y. *Science* **2001**, *392*, 269.
(4) Irie, H.; Watanabe, Y.; Hashimoto, K. *J. Phys. Chem. B* **2003**, *107*, 5483.
(5) Ihara, T.; Miyoshi, M.; Iriyama, Y.; Matsumoto, O.; Sugihara, S. *Appl. Catal. B: Environ.* **2003**, *42*, 403.
(6) Nakamura, I.; Negishi, N.; Kutsuna, S.; Ihara, T.; Sugihara, S.; Takeuchi, K. *J. Mol. Catal. A: Chem.* **2000**, *161*, 205.
(7) Martyanov, I. N.; Uma, S.; Rodrigues, S.; Klabunde, K. J. *Chem. Commun.* **2004**, 2476.
(8) Minero, C.; Mariella, G.; Maurino, V.; Pelizzetti, E. *Langmuir* **2000**, *16*, 2632.
(9) Minero, C.; Mariella, G.; Maurino, V.; Vione, D.; Pelizzetti, E. *Langmuir* **2000**, *16*, 8964.
(10) Vohra, M. S.; Kim, S.; Choi, W. *J. Photochem. Photobiol. A: Chem.* **2003**, *160*, 55.
(11) Yu, J. C.; Yu, J.; Ho, W.; Jiang, Z.; Zhang, L. *Chem. Mater.* **2002**, *14*, 3808.

10.1021/cm049099p CCC: $30.25
Published on Web 04/19/2005

phase photocatalytic system. For the F-doped TiO_2, where the F atoms occupy the crystal sites of the TiO_2 lattice by replacing oxygen atoms, the fluorination proceeded during TiO_2 synthesis.[11] F-doped TiO_2 can be used conveniently for any photocatalytic system.

In this report, the optical properties of the NFT powders prepared by SP were characterized by ultraviolet−visible (UV−Vis) absorption spectroscopy and photoluminescence (PL) spectra. Acetaldehyde decomposition was used as a probe reaction to evaluate the photocatalytic properties of these NFT powders under both UV and Vis irradiation. The effects of N−F-codoping on photocatalytic activity were investigated in detail. The reasons for exhibiting Vis photocatalytic activity in this system were elucidated. These findings are helpful in understanding the role of doped N/F atoms in Vis photocatalysis. Moreover, the potential application of the NFT powders to air purification was also investigated by simulating a commercial LED air cleaner system.

2. Experimental Section

2.1. Synthesis. The N−F−codoped TiO_2 (NFT) powders were prepared by SP from a mixed aqueous solution containing $TiCl_4$ and NH_4F. The detailed process was described in part 1.[1] A series of NFT powders were prepared by changing the SP temperature: they were designated as NFT-xxx, where "xxx" represents the SP temperature in °C. For comparison, undoped SP TiO_2 (T-800) and commercial P25 (Degussa, 50 m^2/g, 75% rutile and 25% anatase) were selected as reference samples.

2.2. Characterization. The UV−Vis spectra were recorded on a Jasco V-550 spectrophotometer with an integrating sphere; $BaSO_4$ was used as a reference sample. The PL spectra were measured at room temperature using an rpm 2000 spectrophotometer (ACCENT Semiconductor Technologies Ltd., UK) with a He−Cd laser (325 nm) as the excitation light source.

2.3. Photocatalytic System. The photocatalytic decomposition of acetaldehyde was carried out in a closed circulation system (CCS) interfaced to a gas chromatograph (G-3900, Hitachi, Japan) for analyses of gas composition. Prior to the catalytic experiments, the NFT powder (0.0500 g) was treated in a flow of oxygen gas at 573 K until no CO_2 product was detected. The sample was then separated from the flow system and switched to the CCS by two three-way stop clocks and evacuated under a vacuum of 10^{-5} Pa at 573 K for 1.0 h. After the sample had cooled to room temperature, a gas mixture of 88.0 kPa He (containing 930 ppm CH_3CHO) and 13.3 kPa O_2 was introduced. The samples were irradiated from outside of the reactor. A 200-W Hg−Xe lamp (LA-300UV, λ_{max} = 365 nm) and a 150-W Xe lamp (LA-254Xe, λ_{max} = 470 nm, Hayashi Watch-Works. Co., Ltd, Japan) were used as the UV and Vis sources, respectively, unless otherwise noted. The Vis wavelength was controlled through a 420-nm cut filter (L42, Kenko, Japan). The incident intensity to the sample surface for both light sources was set to be 20 mW cm^{-2}.

In our study, total carbon amount (TCA, the amount of introduced CH_3CHO) in CCS was checked during and after reaction. The TCA after the reaction was specified in three parts, (1) formed CO_2, (2) undecomposed CH_3CHO, and (3) residual carbon on the surface of the photocatalyst, which was determined by the amount of CO_2 produced from its oxidation at 673 K for 1 h at O_2 atmosphere. If the difference between the TCA and the sum of (1), (2), and (3) is less than 2.5% of the TCA, the obtained reaction data was considered to be believable; otherwise, a repeat experiment was needed.

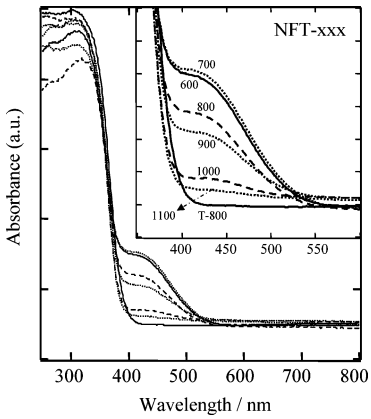

Figure 1. UV−Vis adsorption spectra of NFT powders. The inset shows the enlargement of a part of the adsorption spectra ranging from 350 to 600 nm.

2.4. Acetaldehyde Adsorption. The adsorption experiment was performed volumetrically at 298 K in the same equipment used for the photocatalytic reaction. The adsorbed amount of acetaldehyde on a 0.500 g sample was calculated from the change in acetaldehyde concentration in the gas phase, i.e., subtracting the residual acetaldehyde in the gas phase after the adsorption reached equilibrium from the introduced acetaldehyde (5000 ppm).

3. Results and Discussion

3.1. Optical Characterization. *3.1.1. UV−Vis Spectra.* The absorption spectra of the NFT powders are shown in Figure 1. A new absorption band was observed in the visible range of 400−550 nm in addition to the fundamental absorption edge of TiO_2, which is located in the UV region at about 385 nm. The SP temperature had a strong effect on the Vis absorption intensity, and the maximum VIS absorption was observed from NFT-700. The highest site-N concentration was also achieved in this sample, indicating that Vis absorption is closely related to doped N atoms. Therefore, we attribute the new absorption band to the doped N atoms rather than the doped F atoms because we found that only F-doping did not cause any change in the optical absorption of TiO_2.[12] Other researchers also confirmed that F-doping could not contribute to the optical absorption spectra of TiO_2 by theoretical band calculation.[3,13]

As stated in part 1, the NFT powders were vivid yellow. Generally, the color of a solid is determined by the position of its absorption edge; a shift of this absorption edge toward a higher wavelength can result in absorption in the visible part of the spectrum. For colored nitride compounds, this shift was ascribed to the doped N atoms.[14] Additionally, the adsorption edge of new band (ca. 475 nm) well agree with the reported value for the N-doped TiO_2 system.[2−5] These conclusions strongly support the theory that the appearance of a new absorption band in the visible region over the NFT powders originated from the doped N atoms. However, it should be noted that the doped N atoms exist as an impurity

(12) Li, D.; Haneda, H.; Hishita, S.; Ohashi,N.; Labhsetwar, N. K. *J. Fluorine Chem.* **2005**, *126*, 69.
(13) Yamaki, T.; Umebayashi, T.; Sumita, T.; Yamamoto, S.; Maekawa, M.; Kawasuso, A.; Itoh, H. *Nucl. Instrum. Methods Phys. Res. B* **2003**, *206*, 254.
(14) Marchand, R.; Tessier, F.; Le Sauze, A.; Diot, N. *Int. J. Inorg. Mater.* **2001**, *3*, 1143.

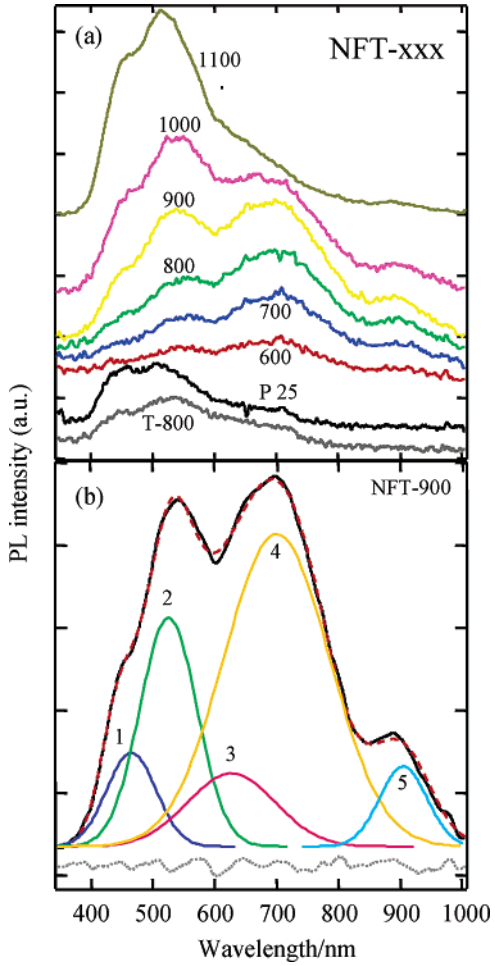

Figure 2. (a) PL spectra of NFT powders and reference samples. (b) Deconvolution of the broad peak for NFT-900. The solid line represents the original TPD profile and deconvoluted peaks, the broken line is the fitting curve, and the dotted line is the error of the fitting.

since its concentration was too low to form a new phase to cause a shift of the fundamental absorption edge of TiO_2, as observed in a TiO_xN_y thin film.[15]

3.1.2. PL Spectra. PL emission spectra have been widely used to investigate the efficiency of charge carrier trapping, migration, and transfer and to understand the fate of electron−hole pairs in semiconductor particles.[16] Figure 2a shows the PL spectra of the NFT powders as well as reference samples. A broad band including more than four peaks was observed for each NFT powder. Accordingly, the PL spectrum of each NFT powder was deconvoluted into five peaks; an example is shown in Figure 2b for NFT-900. Peak 1 at 465 nm is attributed to the oxygen vacancy with two trapped electrons, i.e., *F* center. Peak 2 at 525 nm is assigned to the oxygen vacancy with one trapped electron, i.e., F^+ center.[17−19] Peak 3 at 627 nm might be a consequence of the Franck−Condon principle and the polarizability of

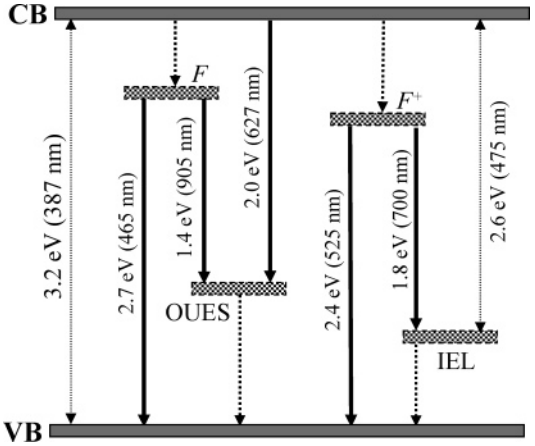

Figure 3. Proposed structural model of energy states that exist between the VB and CB of TiO_2. The dotted arrows represent the possible existing PL emissions beyond 1000 nm.

the lattice ions surrounding the vacancy; the emitting center was identified as Ti^{3+} ions.[20] However, the energy state induced by Ti^{3+} ions seems to locate just below the CB of TiO_2.[11] Therefore, in this study, peak 3 is considered as an origin-unidentified peak. Peak 4 at 700 nm is attributed to the doped N atoms because no such peak was found on T-800 and P25. The PL intensity increased monotonically with the SP temperature, indicating that the radiative recombination was enhanced with the SP temperature. This enhancement is mainly attributed to the doped F atoms because we found a similar result on a TiO_2 system doped only with fluorine.[12]

PL spectra also directly reveal the processes of the radiative recombination of charge carriers between two different energy states.[17] In the case of NFT powders, shallow traps exist at 0.51 and 0.82 eV below the CB, corresponding to peak 1 and peak 2, respectively. These values agree well with the reported *F* and F^+ center levels in TiO_2.[17−19] A deep trap also exists at 2.0 eV below the CB corresponding to peak 3; its energy state is denoted as OUES, origin-unidentified energy state. Additionally, the UV−Vis spectra in Figure 1 indicate that the doped N atoms formed an impurity energy state (IES) (2.6 eV, 475 nm) below the CB, although a peak concerning the transition between CB and IES did not show up in the PL spectra. This disagreement between the UV−Vis and PL spectra is easy to be understood because the appearance of light absorption between two different energy states does not mean the inevitable presence of a photoluminescence emission. Therefore, only by the combination of UV−Vis and PL spectra can the energy states between the VB and CB be entirely elucidated.

Based on these results, we propose a structural model in Figure 3 for the energy states existing between the VB and CB of N−F−codoped TiO_2. The excited electron transition pathways corresponding to each peak is also depicted. The peak 4 is assigned to the transfer of excited electrons between F^+ center and IES. Peak 5 at 905 nm is assigned to the transfer of excited electrons between *F* center and OUES. Here, we would like to emphasize the presence of oxygen vacancies because many studies have confirmed that the

(15) Matin, N.; Banakh, O.; Santo, A. M. E.; Springer, S.; Sanjinés, R.; Takadoum, J.; Lévy, F. *Appl. Surf. Sci.* **2001**, *185*, 123.
(16) Yamashita, H.; Ichihashi, Y.; Zhang, S. G.; Matsumura, Y.; Souma, Y.; Tatsumi, T.; Anpo, M. *Appl. Surf. Sci.* **1997**, *121*, 305.
(17) Serpone, N.; Lawless, D.; Khairutdinov, R. *J. Phys. Chem.* **1995**, *99*, 16646.
(18) Saraf, L. V.; Patil, S. I.; Ogale, S. B.; Sainkar, S. R.; Kshirsager, S. T. *Int. J. Mod. Phys. B* **1998**, *12*, 2635.
(19) Lei, Y.; Zhang, L. D.; Meng, G. W.; Li, G. H.; Zhang, X. Y.; Liang, C. H.; Chen, W.; Wang, S. X. *Appl. Phys. Lett.* **2001**, *78*, 1125.
(20) Ghosh, A. K.; Wakim, F. G.; Addiss, R. R., Jr. *Phys. Rev.* **1969**, *184*, 979.

Table 1. Photocatalytic Activities of NFT Powders

sample	NFT-600	NFT-700	NFT-800	NFT-900	NFT-1000	NFT-1100	T-800	P25
$R_0/10^{-7}$ mol min^{-1} (UV)	4.04	5.32	6.44	10.3	8.24	1.21	1.20	6.74
QY/%(UV)	2.5	2.9	3.3	4.2	3.7	1.7	1.0	3.5
$R_0/10^{-8}$ mol min^{-1} (Vis)	2.46	3.45	4.35	8.41	5.53	0.61	0.12	1.2
QY/% (Vis)	0.28	0.39	0.47	0.78	0.60	0.086	0.015	0.14

formation of the superoxide ($O_2^{\bullet-}$) and hydroxyl ($OH^{\bullet}$) radicals, two important active species for initiating a photocatalytic reaction,[21,22] requires oxygen vacancy sites.[23,24]

3.2. Photocatalysis. *3.2.1. UV Photocatalytic Decomposition of Acetaldehyde.* The CO_2 evolution during acetaldehyde decomposition on the NFT powders under UV irradiation is shown in Figure 4. The photocatalytic activity of the NFT powders greatly depended on the SP temperature. The maximum photocatalytic activity was observed for NFT-900, and it was higher than that of P25. Generally, many factors, e.g., surface area, crystallinity, surface hydroxyl density, and oxygen vacancies, affect the activity of a photocatalyst.[25,26] However, because these factors are closely related to each other, e.g., the surface area decreases with an increase in crystallinity by calcination, it is difficult in practice to control each factor precisely and independently for obtaining the highest photocatalytic activity. Thus, the activity of a photocatalyst is a combined effect of many factors.[27] In our case, the SP temperature used during the sample preparation process dominated these factors because other preparation conditions were identical. Therefore, it is easy to understand that the highest photocatalytic activity was achieved at a particular SP temperature.

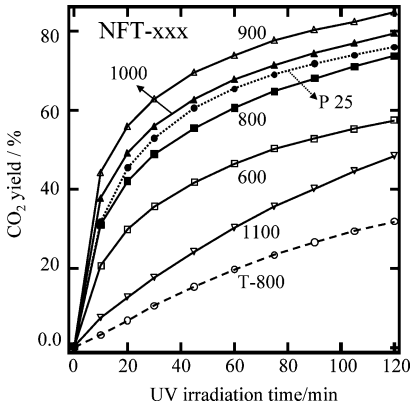

Figure 4. CO_2 evolution during the UV photocatalytic decomposition of acetaldehyde on NFT powders.

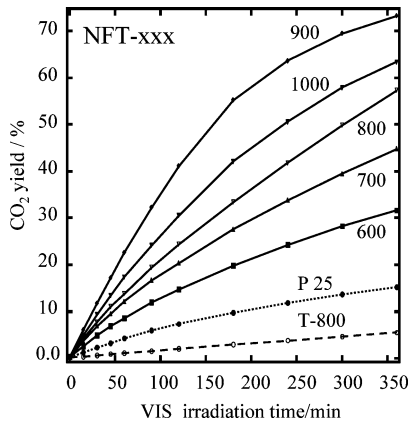

Figure 5. CO_2 evolution during the Vis photocatalytic decomposition of acetaldehyde on NFT powders.

In this study, the initial rate (R_0, mol min^{-1}) and quantum yield (QY, %) of CO_2 formation, 1.0 h after the reaction began, were calculated to represent the photocatalytic activity in order to make a quantitative comparison. The results are summarized in Table 1. R_0 value is a product of the slope of the time−CO_2 yield curve (Figure 4) at time = 0 and a constant. The constant is the upper-limit amount of potentially formed CO_2, which is twice the amount of introduced CH_3CHO. QY is a ratio of the number of formed CO_2 molecules to the number of consumed photons.[28] The photocatalytic activity of NFT-900 was higher than that of P25 by 1.5 times for R_0 and 1.2 times for QY. When a material is functionalized for Vis-driven photocatalysis, it is important to keep or improve its UV photocatalytic activity because the most desired solar light source contains about 5% UV and the efficiency of light utilization for a TiO_2-based photocatalyst is much higher for UV than for Vis.[12] Comparing the photocatalytic activities of NFT-800 and T-800 prepared at the same SP temperature, we concluded that the photocatalytic activity of the former was higher than the latter by 5.3 times for R_0 and 3.3 times for QY. The unique surface structure and the doped F atoms were considered to contribute for the high UV photocatalytic activity of NFT-900.

3.2.2. Vis Photocatalytic Decomposition of Acetaldehyde. The CO_2 evolution over the NFT powders with Vis irradiation at wavelengths longer than 420 nm is given in Figure 5. The results are similar to those of the UV case. However, it should be noted that each NFT powder demonstrated a higher photocatalytic activity compared with P25, indicating that N−F-codoping is an effective and feasible approach for achieving Vis-driven photocatalysis. The R_0's and QY's of CO_2 formation, 3 h after the reaction began, are listed in Table 1. The photocatalytic activity of NFT-900 was higher than that of P25 by 7.0 times for R_0 and 5.7 times for QY. Comparing the photocatalytic activities of NFT-800 and T-800, we concluded that the photocatalytic activity of the former was higher by 36 times for R_0 and 31 times for QY than that of the latter. The Vis-driven photocatalysis induced by the N−F-codoping is outstanding.

To elucidate the correlation between the photocatalytic activity and the site-N/F concentrations, the site-N/F con-

(21) Mills, A.; Hunte, S. L. *J. Photochem. Photobiol. A: Chem.* **1997**, *108*, 1.
(22) Fujishima, A.; Rao, T. N.; Tryk, D. A. *J. Photochem. Photobiol. C: Photochem. Rev.* **2000**, *1*, 1.
(23) Henderson, M. A.; Epling, W. S.; Perkins, C. L.; Peden, C. H. F. *J. Phys. Chem. B* **1999**, *103*, 5328.
(24) Schaub, R.; Thostrup, P.; Lopez, N.; Lægsgaard, E.; Stensgaard, I.; Nørskov, J. K.; Besenbacher, F. *Phys. Rev. Lett.* **2001**, *87*, 266104.
(25) Fox, M. A.; Dulay, M. T. *Chem. Rev.* **1993**, *93*, 341.
(26) Li, D.; Haneda, H. *Chemosphere* **2003**, *51*, 129.
(27) Li, D.; Haneda, H. *J. Photochem. Photobiol. A: Chem.* **2003**, *160*, 203.
(28) Sopyan, I.; Watanabe, M.; Murasawa, S.; Hashimoto, K.; Fujishima, A. *J. Photochem. Photobiol. A: Chem.* **1996**, *98*, 79.

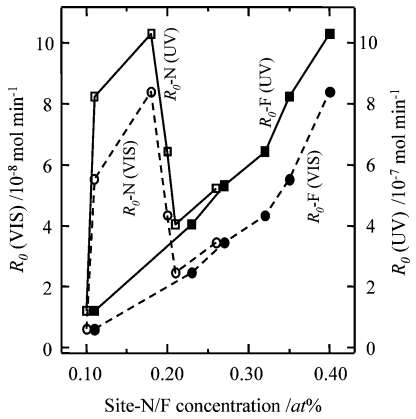

Figure 6. Dependence of the photocatalytic activity on the site-N/F concentration.

centration values in the NFT powders, given in part 1,[1] were arranged in magnitude order. Then the arranged site-N/F concentration values were designed as abscissa, and the R_0 values of the NFT powders that every site-N/F concentration value corresponded to were designed as ordinate. Consequently, Figure 6 was obtained. No correlation between the R_0's and the site-N concentrations was observed for both UV and Vis cases. This is ascribed to the double-faced behaviors of the doped N atoms. Except for the positive roles, to be discussed later, the IES formed upon N-doping (Figure 3) also acts as a recombination center of photogenerated charge carriers, and thus deteriorates photocatalysis.[4] However, the R_0 value monotonically increased with the increase of the site-F concentration irrespective of UV or Vis case. This confirms that the doped F atoms contributed the Vis photocatalytic activity of the NFT powders.

3.2.3. Potential Application to Air Purification. An LED (light-emitting diode) air cleaner for use in cars is a typical example of a practical application of photocatalytic technology to air purification. The LED is characterized by low powder consumption, semi-permanent lifetime, quick response time, and small volume compared with conventional light sources.[29] Therefore, it is said that LED is so far the most desired light source for a photocatalytic system from an energy-saving point of view; its application in photocatalytic systems will significantly stimulate the implementation of photocatalytic technology. Here, we simulated this system and designed a special reactor cell with an interior LED (λ_{max} = 470 nm) (Figure 7) to investigate the potential application of our SP samples. Besides acetaldehyde, trichloroethylene and toluene were selected as the other two target reactants. Each reactant was carried with water-free synthesized air (N_2/O_2 = 79/21, v/v). The total carbon amounts introduced to the reaction system for the three reactants were designed to be at the same level in order to compare their degrees of decomposition.

The results are given in Figure 8. NFT-900 demonstrated a powerful photocatalysis, and its photocatalytic activity was superior to that of commercial TiO_2 P25 for each of the target reactants. Six hours after the reaction started, the CO_2 yield was 54.8% for acetaldehyde, 33.0% for trichloroethylene,

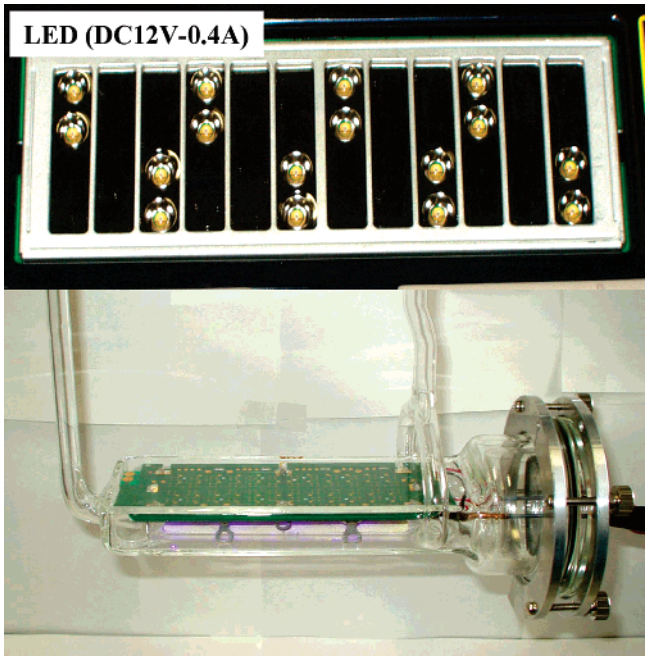

Figure 7. Designed photocatalytic reactor cell with an interior blue LED light source.

and 13.7% for toluene, indicating that acetaldehyde is the easiest reactant to be decomposed and toluene is the most difficult. Additionally, the very slow CO_2 evolution in the blank test (no photocatalyst) confirmed that the decompositions of the three typical air pollutants occurred through photocatalysis and that their self-photolysis could be neglected.

Here, it should be noted that trichloroethylene and toluene are generally degraded into CO_2 only under high-energy UV irradiation.[30,31] However, they decomposed over our SP samples under Vis irradiation. Moreover, we used a very high concentration for each pollutant. Generally, their concentrations are much lower in polluted air; e.g., the upper limit of toluene concentration in indoor air is 0.07 ppm if Japanese indoor environmental regulations are being complied with, and it would be only 7 ppm even if it exceeds this specified value by 100 times. Therefore, we think that our SP samples have a good potential for application to air purification.

3.2.4. Possible Reasons for the High Photocatalytic Activity of the NFT Powders. The NFT powder demonstrated a high photocatalytic activity under both UV and Vis irradiation. The reasons should be closely related to its unique surface characteristics, the doped N atoms, and the doped F atoms. First, the highly porous and strongly acidic surface enhanced the adsorptivity of the NFT powder for a reactant. The dependence of the adsorbed amount of acetaldehyde (A_{ad}) on surface acidity on the NFT powders is shown in Figure 9. The A_{ad} almost linearly increased with the surface acid site density except NFT-1100, suggesting that the acidic surface of the NFT powders is beneficial for the adsorption of reactant molecules. The A_{ad} of NFT-900 (15.2 μmol m^{-2}) was much higher than that of P25 (8.6 μmol m^{-2}). Kwan et

(29) Taoda, H., Ed. *Book on Photocatalysis*; Nikan kougyou: Tokyo, 2002; p 124.

(30) Zou, G. M.; Cheng, Z. X.; Xu, M.; Qiu, X. Q. *J. Photochem. Photobiol. A: Chem.* **2003**, *161*, 51.

(31) Jeong, J.; Sekiguchi, K.; Sakamoto, K. *Chemosphere* **2004**, *57*, 663.

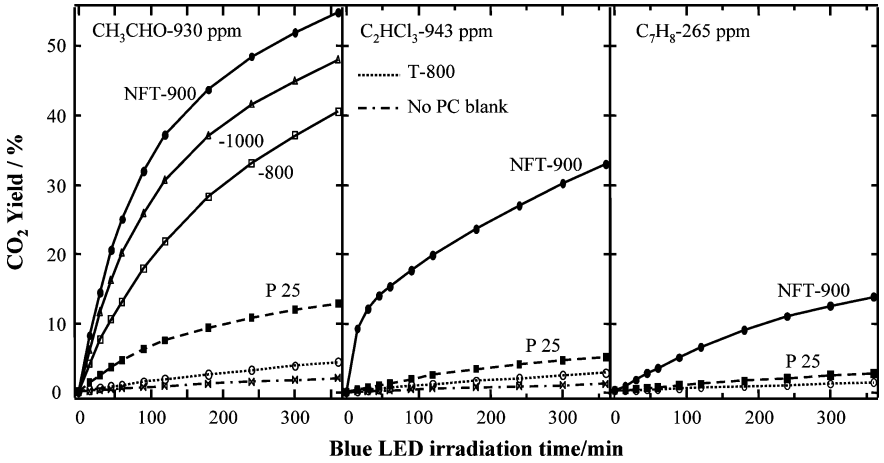

Figure 8. CO_2 evolution during the photocatalytic decomposition of three air pollutants on NFT-900 and reference samples when the LED was used as a light source. The tested photocatalyst was 0.500 g.

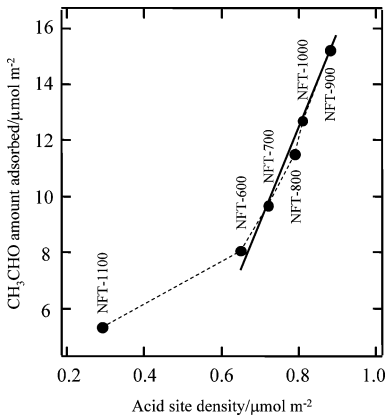

Figure 9. Dependence of the absorbed amount of acetaldehyde on the surface acidity on NFT powders.

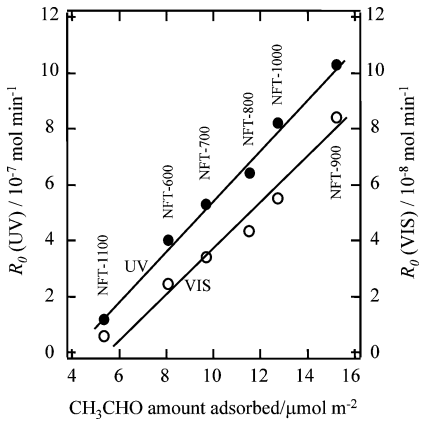

Figure 10. Dependence of the photocatalytic activity on the absorbed amount of acetaldehyde on NFT powders.

al. confirmed that the enhancement in surface acidity improves the activity of a photocatalytic system.[32]

The dependence of the photocatalytic activity (R_0) on the A_{ad} is given in Figure 10. A linear relationship between the R_0 and A_{ad} was observed irrespective of UV or Vis irradiation, indicating that A_{ad} is a key factor affecting the R_0. Generally, the reaction rate (r) of a photocatalytic reaction can be described by Langmuir−Hinshelwood kinetic equation:[32]

$$r = kKC/(1 + KC) \quad (1)$$

where K is the adsorption coefficient of the reactant, which is closely related to the microstructure of the particle surface, e.g., surface area and acidity; k represents the reaction rate constant, which is closely connected with the density of space-separated electrons and holes that appeared on the surface of a photocatalyst; C denotes the concentration of the reactant to be decomposed. Therefore, to provide high photocatalytic efficiency, a photocatalyst must retain large K and k values. In our case, a large A_{ad} means a large K; thus, the R_0's of the NFT powders linearly increased with the surface acidity. Moreover, the surface acidic site also acts as an electron acceptor.[33] This would enhance the separation of photogenerated electrons and holes, i.e., increase k value, and improve the photocatalytic activity.

Second, the doped N atoms in the NFT powders improved the Vis absorption. The UV−Vis spectra in Figure 1 unequivocally indicate that the N-doping did not cause the narrowing of the band gap of the TiO_2 in our NFT system because a shift in the fundamental absorption edge of TiO_2 was not observed. Instead, an isolated impurity energy state (IES, Figure 3) was formed near the VB of the TiO_2. The presence of this IES improved the Vis absorption and increased the number of photons taking part in the photocatalytic reaction. Undoubtedly, this could enhance the photocatalytic activity. Moreover, the formation of oxygen vacancies upon N-doping is considered in terms of the charge neutrality conditions. Incorporation of the two N atoms into the oxygen sites should be accompanied by the formation of one oxygen vacancy to maintain the overall electroneutrality of the crystal lattice. However, in the NFT system, it appears that the contribution of the doped N atoms to the Vis photocatalytic activity through the oxygen vacancies was not significant. This was inferred from our results showing a much higher photocatalytic activity for the N−F−codoped TiO_2 powders than for the N-doped TiO_2.[34] Therefore, the contribution of the doped N atoms to the Vis photocatalytic activity in our NFT system is achieved mainly by the improvement of the Vis absorption.

(32) Kwon, Y. T.; Song, K. Y.; Lee, W. I.; Chio, G. J.; Do, Y. R. *J. Catal.* **2000**, *191*, 192.
(33) Morrison, S. R. *Surf. Sci.* **1975**, *50*, 329.
(34) Li, D.; Haneda, H.; Hishita, S.; Ohashi, N. *Mater. Sci. Eng. B* **2005**, *117*, 67.

Third, the doped F atoms in NFT powders produced several beneficial effects on the photocatalytic activity which are listed below. (1) F-doping led to the formation of new active sites. Our PL results in Figure 2 indicated that F-doping mainly contributed to the formation of oxygen vacancies (*F* and F^+ centers). As stated above, the formation of the $O_2^{\bullet-}$ and $OH^\bullet$ radicals requires oxygen vacancy sites.[23,24] Emeline et al. also elucidated in detail the enhanced effect of oxygen vacancies (including *F* and F^+ centers) on photocatalysis.[35] If the oxygen vacancy acts as a site for the formation of the active radicals, F-doping undoubtedly increases the number of this kind of active sites. Minero et al. claimed that the formation of hydroxyl radicals ($OH^\bullet$) was favored on fluorinated TiO_2.[8,9] This also indirectly supports the role of new active sites formed by doped F atoms. (2) F-doping resulted in the formation of surface acid sites. These acid sites would not only increase the adsorptivity of the NFT powders for a reactant but also act as electron acceptors by themselves. (3) It was reported that F-doping increased the photogenerated electron mobility in TiO_2.[36] Therefore, the photogenerated electrons in the NFT powders could easily diffuse from the inner region to the surface of the particles to take part in the surface photochemical reaction.

Consequently, the high Vis photocatalytic activity of NFT powder is ascribed to a synergetic effect of its unique surface characteristics, doped N atoms, and doped F atoms. The porous and acidic surface enhanced its adsorptivity to reactant molecules; the doped N atoms improved the visible-light absorption; and the doped F atoms could produce several beneficial effects on the photocatalytic activity. However, for the case of UV, the doped N atoms might have a negative effect since they led to the formation of the IES that could act as a recombination center of photogenerated charge carriers.

4. Conclusions

The N−F−codoped TiO_2 powder demonstrated a higher photocatalytic activity under both UV and Vis irradiation as compared to undoped SP TiO_2 as well as commercial P25. This high activity was ascribed to a synergetic effect of its unique surface characteristics, doped N atoms, and doped F atoms. The simulation results indicate that our NFT powder is a very interesting and promising photocatalytic material and has good potential for application to air purification.

Acknowledgment. This research is part of the Millennium Project for the "Search and Creation of a Catalyst for Removing Harmful Chemical Substances" sponsored by the Ministry of Education, Culture, Sports, Science and Technology (MEXT), Japan. It was also supported by the Industrial Technology Grant Program (ID04A26018) from the New Energy and Industrial Technology Development Organization (NEDO), Japan. Here, we are grateful for the financial support. The LED panel used in this study was provided by Koha Co., Ltd., Japan, who we also thank for their cooperation.

CM049099P

(35) Emeline, A. V.; Kuzmin, G. N.; Purevdorj, D.; Ryabchuk, V. K.; Serpone, N. *J. Phys. Chem. B* **2000**, *104*, 2989.
(36) Subbarao, S. N.; Yun, Y. H.; Kershaw, R.; Dwighta, K.; Word, A. *Inorg. Chem.* **1979**, *18*, 488.